

## Article

# Nonlinear Settlement Calculation of Composite Foundation Based on Tangent Modulus Method: Two Case Studies

Yonghua Li <sup>1,\*</sup>, Lei Yao <sup>1</sup>, Gaoxiang Chen <sup>1</sup>, Weijian Zhao <sup>1</sup> and Xiangang Liu <sup>2</sup>

<sup>1</sup> School of Infrastructure Engineering, Nanchang University, Nanchang 330031, China; 406000210032@email.ncu.edu.cn (L.Y.); 416000210080@email.ncu.edu.cn (G.C.); 416000210034@email.ncu.edu.cn (W.Z.)

<sup>2</sup> JiangXi Jiye Science and Technology Group Co., Ltd., Nanchang 330013, China; 13970032360@139.com

\* Correspondence: liyonghua@ncu.edu.cn

**Abstract:** The tangent modulus method of undisturbed soil is a new method in settlement calculation, which is mainly applied to hard soil with a strong structure, such as silty clay, completely weathered rock, and granite residual soil with an SPT blow count greater than 8. The tangent modulus is mainly obtained from a field plate load test, which can consider the influence of the soil stress level and reflect the nonlinear characteristics of the foundation settlement. In a multi-layer soil foundation, since the deep plate loading test is difficult, a method was proposed to determine the tangent modulus of deep soil. It is assumed that the ratio of the initial tangent modulus to the deformation modulus is equal to the ratio of the unloading–reloading modulus  $E_{ur}^{ref}$  to the secant modulus  $E_{50}^{ref}$  obtained by triaxial unloading–reloading test. Since there are corresponding empirical formulae for SPT counts and the deformation modulus of different types of soils in many regions, the initial tangent modulus can be derived by the above method. In two cases of a composite foundation, the compression modulus and tangent modulus were used to calculate the settlement of the foundation, which is then compared with the measured results. The results show that the proposed method for determining the tangent modulus of deep soil is feasible in theory, and the calculating accuracy of the tangent modulus is significantly higher than that of the traditional compression modulus.

**Keywords:** multi-layer soil foundation; nonlinear settlement; tangent modulus; deformation modulus

**Citation:** Li, Y.; Yao, L.; Chen, G.; Zhao, W.; Liu, X. Nonlinear Settlement Calculation of Composite Foundation Based on Tangent Modulus Method: Two Case Studies. *Buildings* **2023**, *13*, 892. <https://doi.org/10.3390/buildings13040892>

Academic Editor:  
Gianfranco De Matteis

Received: 19 January 2023  
Revised: 20 March 2023  
Accepted: 24 March 2023  
Published: 28 March 2023



**Copyright:** © 2023 by the authors. Licensee MDPI, Basel, Switzerland. This article is an open access article distributed under the terms and conditions of the Creative Commons Attribution (CC BY) license (<https://creativecommons.org/licenses/by/4.0/>).

## 1. Introduction

The calculation of the foundation settlement is an ancient problem in soil mechanics, which has not been solved well at present. The settlement of the foundation is affected by the stiffness of the foundation and the characteristics of the soil. When the soil is reinforced, the mechanical characteristics of the composite foundation are more complex. Zhang [1] studied the calculation of the settlement of foundations reinforced with a gravel pier and proposed an analytical solution for the settlement based on this deformation characteristic. Chang [2] used the three-dimensional finite element method to study the load response mechanism of the foundation in clay and sand. Pantelidis [3] studied the relationship between the settlement of rigid rectangular foundations and corresponding flexible foundations. Wang [4] used the equivalent soil modulus and weighted soil modulus to analyze the settlement of the CFG pile and ram-compaction pile composite foundation, respectively, and pointed out that the equivalent soil modulus is more suitable for the settlement calculation of the composite foundation.

The layerwise summation method based on the soil compression modulus was generally adopted to calculate the foundation settlement in China. The compression modulus of the soil layer is generally measured in a laboratory test. Theoretically, the compression modulus is greater than the deformation modulus. However, for low-compressibility soils, the measured deformation modulus is much larger than the compression modulus

due to sampling disturbances in laboratory tests sometimes. Yang [5] pointed out that the deformation modulus of granite residual soils obtained in the field load test is often 6–10 times higher than the compression modulus in the Guangdong region of China, and the calculated settlement of the foundation with the compression modulus is much larger than the measured settlement.

In addition, the deformation modulus of the soil is also related to its stress level. Based on the Duncan–Chang model [6], Yang [5,7–9] proposed the tangent modulus method for the nonlinear settlement calculation. According to the in-situ load plate test curves, the relation of the tangent modulus of the soil with the stress level was set up and the tangent modulus of different-depth soil could be computed based on its stress level. In the Chinese Code for the Design of Building Foundations [10], the calculated value of the settlement needs to be corrected by the empirical coefficient, but the tangent modulus method does not need to use the empirical coefficient in the calculation of the settlement, which avoids the disadvantage where the value of the empirical coefficient is affected by the experience of the engineer.

Due to the complexity and high cost of the deep plate load test, a method to determine the tangent modulus of deep soil is proposed, which uses a field standard penetration test and triaxial test of the sampled soil to obtain the tangent modulus of deep soil. Based on two multi-layer soil composite foundation cases, the settlement calculation is carried out using the tangent modulus and compared with the measured settlement to verify the feasibility of the derivation of the tangent modulus in the deep soil layer.

## 2. Calculation Principle of Tangent Modulus Method

### 2.1. Settlement Calculation Method of Composite Foundation—Layerwise Summation Method

The layerwise summation method is used to calculate the natural foundation settlement in the Chinese Code for the Design of Building Foundations [10], and the deformation of the foundation can be calculated according to the following formula:

$$s = \psi_s s' = \psi_s \sum_{i=1}^n \frac{p_0}{E_{si}} (z_i \bar{\alpha}_i - z_{i-1} \bar{\alpha}_{i-1}) \quad (1)$$

where  $s$  is the final deformation of the foundation, and  $s'$  is the foundation deformation calculated by the layerwise summation method;  $\psi_s$  is the settlement calculation empirical coefficient, which is shown in Table 1;  $n$  is the number of soil layers in the depth range of the foundation deformation calculation;  $p_0$  is the additional pressure.  $E_{si}$  is the modulus of the compression of the  $i$ th layer;  $z_i$  is the depth of the  $i$ th layer of soil; and  $\bar{\alpha}_i$  is the average additional stress coefficient.

According to the Technical Code for Building Foundation Treatment [11], the settlement of the composite foundation after dynamic compaction is still calculated by the layerwise summation method, and the equivalent compression modulus  $E_{sp}$  of the composite soil layer can be obtained as follows:

$$E_{sp} = \zeta E_s = \frac{f_{spk}}{f_{ak}} E_s \quad (2)$$

where  $f_{spk}$  is the characteristic value of the bearing capacity of the composite foundation, and  $f_{ak}$  is the characteristic value of the natural foundation.

$\bar{E}_s$  is the equivalent value of the compression modulus in the depth range for the deformation calculation, which is calculated as follows:

$$\bar{E}_s = \sum A_i / \sum \frac{A_i}{E_{si}} \quad (3)$$

where  $A_i$  is an integral value of the additional stress coefficient of the  $i$ th layer of soil along the soil depth.

**Table 1.** Empirical coefficient of calculated settlement  $\psi_s$ .

$\overline{E}_s$ (MPa)	4	7	15	20	35
$\psi_s$	1	0.7	0.4	0.25	0.2

## 2.2. Tangent Modulus of Shallow Soil

Considering the great difference between the parameters of the disturbed soil and the in-situ soil, the tangent modulus method for the nonlinear settlement of the foundation was proposed by Professor Yang [5]. Assuming the load–settlement  $p$ – $s$  curve can be fitted by hyperbola  $p = \frac{s}{a + bs}$ , and according to the Boussinesq solution for the soil settlement under uniform load, the initial tangent modulus of the soil can be obtained as follows [5]:

$$E_{t0} = \frac{D(1 - \mu^2)\omega}{a} \quad (4)$$

where  $E_{t0}$  is the initial tangent modulus of the undisturbed soil;  $D$  is the diameter of the plate in the test;  $\mu$  is the Poisson's ratio of the soil;  $\omega$  is the settlement influence coefficient, which is related to the shape of the loading plate; and  $a$  is the parameter of the hyperbolic curve.

Further, the tangent modulus equation between the tangent modulus and the stress of the soil under a different additional load  $p$  can be obtained [5]:

$$E_t = \left(1 - R_f \frac{p}{P_u}\right)^2 E_{t0} \quad (5)$$

where  $P_u$  is the ultimate bearing capacity, and  $b$  is a hyperbolic fitting parameter with  $b = 1/p_u$ .  $R_f$  is the damage ratio coefficient, and  $E_t$  is the tangent modulus of the soil under a different stress level.

## 2.3. Tangent Modulus of Deep Soil

Figure 1 shows the stress–strain relationship curve of the soil in a standard triaxial drainage unloading–reloading test [12–14]. The secant modulus  $E_{50}^{\text{ref}}$  is the ratio of stress to strain when the soil stress reaches half of the failure stress (the characteristic value of the bearing capacity). In the unloading stage, the stress–strain curves do not return to the origin, and the elastic deformation can be restored, while the plastic deformation cannot. The unloading–reloading process of the soil can be expressed by the unloading–reloading modulus  $E_{\text{ur}}^{\text{ref}}$ . The proportion of  $E_{\text{ur}}^{\text{ref}}$  and  $E_{50}^{\text{ref}}$  can be derived by the triaxial drainage unloading–reloading test.

Assuming the ratio of the initial tangent modulus to the deformation modulus is the same as the ratio of the unloading–reloading modulus  $E_{\text{ur}}^{\text{ref}}$  to the secant modulus  $E_{50}^{\text{ref}}$ , when the deformation modulus of deep soil is determined by the SPT blow count, the initial tangent modulus can be derived according to the ratio.

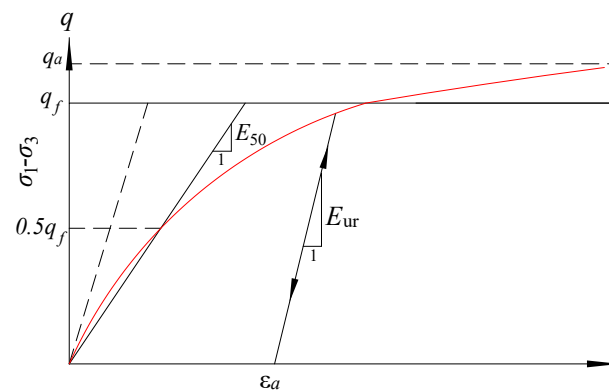


Figure 1. Unloading–reloading stress–strain curves.

### 3. Test Case 1—Settlement of Multi-Layer Soil Composite Foundation

#### 3.1. Project Profile

The 9# high-rise residential building with a shear wall structure is located in Jiujiang City, with 28 floors above ground and one basement. The typical geological profile is shown in Figure 2, and the raft foundation is located at  $-4.2$  m. According to the laboratory soil and field standard penetration test, the physical and mechanical properties of each soil layer are shown in Table 2, where  $c$  is the cohesion,  $\varphi$  is the internal friction angle, and  $N$  is the SPT blow count.

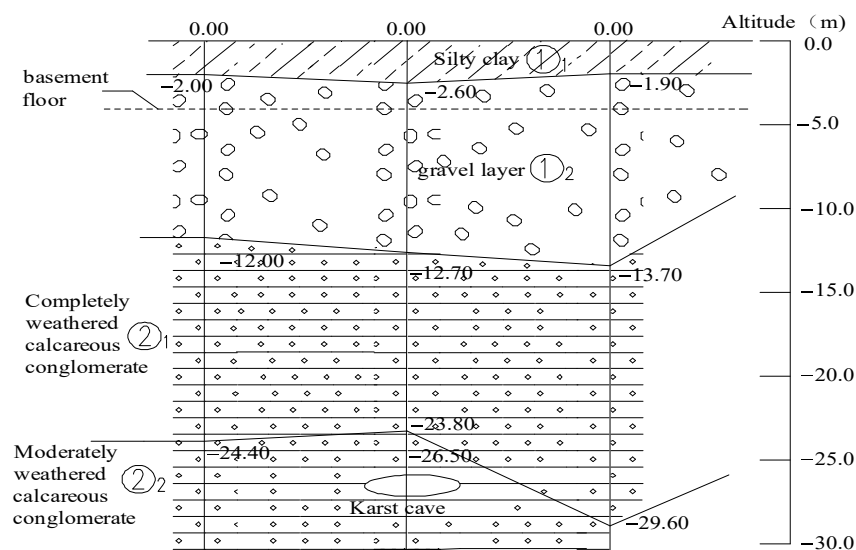


Figure 2. Typical geological profile of 9# building.

Table 2. Physical and mechanical parameters of soils.

Soil Layer	Poisson's Ratio $\mu$	Gravity (kN/m <sup>3</sup> )	Characteristic Value $f_{ak}$ (kPa)	Modulus of Compression $E_s$ (MPa)	$C$ (kPa)	$\varphi$ (Degrees)	SPT Blow Count $N$
Silty clay	0.3	18.8	130	5.91	17	15.61	6
Gravel layer	0.24	20.5	340	27	0	34	(12)
Completely weathered calcareous conglomerate	0.26	19.5	210	15	32	20	16

Note: The number with parentheses is dynamic penetration blow count.

It can be seen from Table 2 that the characteristic value of the bearing capacity of the gravel layer and completely weathered calcareous conglomerate are 340 kPa and 210 kPa, respectively, and the compression modulus of the gravel layer is 27 MPa, which is greater than 15 MPa of the completely weathered calcareous conglomerate.

A raft foundation of 1.4 m thickness was adopted in the 9# residential building. The layout of the shear wall and raft slab foundation is detailed in Figure 3. The bearing capacity of the composite foundation after treatment is required to reach a characteristic value of 420 kPa. First of all, the natural foundation was treated by column hammer dynamic compaction with the space of 2.2 m, then a flat hammer was used for ramming the whole site. Figure 3 also shows the layout of the dynamic compaction points and the boundary of the composite foundation, which extends 3 m from the raft boundary, and Figure 4 shows the construction photos of the dynamic compaction operation with the column hammer and flat hammer.

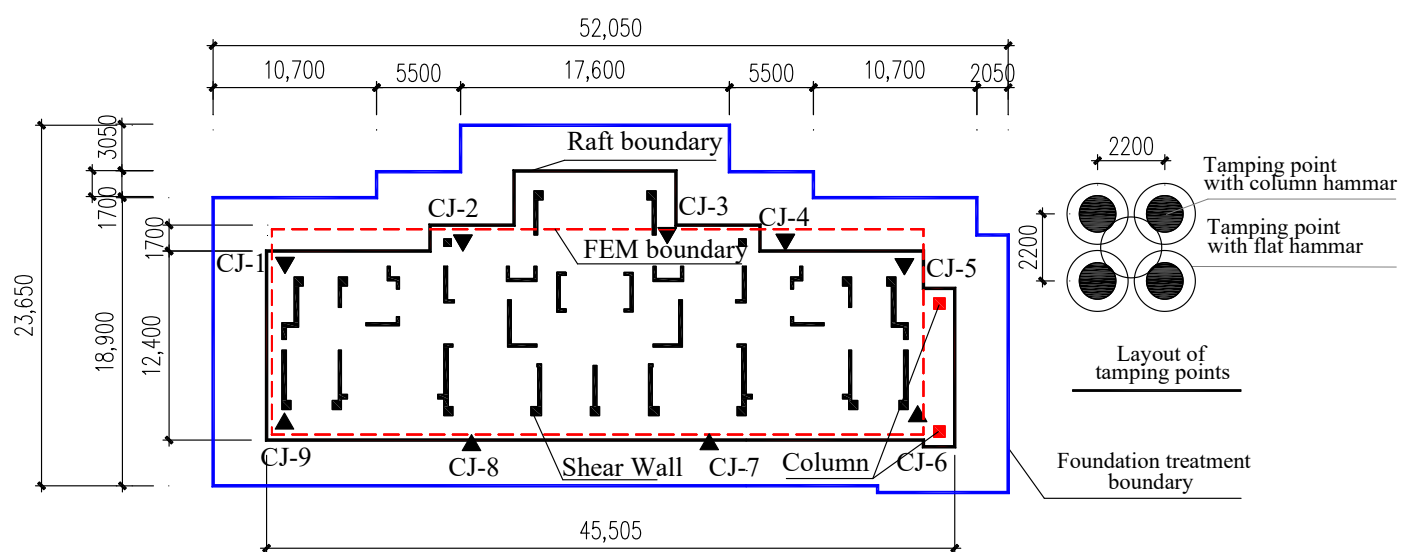


**Figure 3.** Layout of foundation and settlement monitoring points of 9# building.



**Figure 4.** Construction photo of combined hammer: (a) flat hammer; and (b) column hammer.

According to the Chinese Code for Deformation Measurement of Building and Structure [15], nine monitoring points are arranged around the building for settlement monitoring. The monitoring points are arranged on the shear wall of the main structure, as shown in Figure 3. Table 3 shows the settlement values of the monitoring points from the construction to the 7th, 14th, 21st, and 28th floors. During construction, the load of each layer of the structure is about 12 kN/m<sup>2</sup>.

It can be seen from Table 3 that after the completion of the main structure, the measured settlements at the right corner points CJ5 and CJ6 are 15.8 mm and 15.3 mm, respectively, and the measured settlements at the left corner points CJ1 and CJ9 are 10.35 mm

and 10.30 mm, respectively. The settlement of the right corner is significantly greater than that of the left corner. The reason is that there is a two-storey annex on the right side of the 9# building, and two columns of the annex are supported on the raft, which increases the internal force of the raft. The measured settlements of CJ3 and CJ7 at the midpoint of the boundary line are 14.85 mm and 15.42 mm, respectively. To sum up, the settlements at the midpoint of the boundary line are significantly greater than that at the corner.

**Table 3.** Settlement of monitoring point.

Monitoring Point	Cumulative Settlement (mm)			
	Construction to the 7th Floor (84 kN/m <sup>2</sup> )	Construction to the 14th Floor (168 kN/m <sup>2</sup> )	Construction to the 21st Floor (252 kN/m <sup>2</sup> )	Construction to the 28th Floor (336 kN/m <sup>2</sup> )
CJ-1	1.69	3.21	5.01	10.35
CJ-2	1.74	3.33	6.20	12.18
CJ-3	1.72	3.39	7.96	14.85
CJ-4	1.52	3.22	7.35	14.79
CJ-5	1.76	3.31	7.31	15.80
CJ-6	1.68	3.42	6.66	15.30
CJ-7	1.61	3.32	7.00	15.42
CJ-8	1.74	3.25	5.05	10.87
CJ-9	1.65	3.39	4.91	10.30

### 3.2. Vertical Static Load Test of Dynamic Compaction Composite Foundation

A plate loading test was conducted on the composite soil, and the plate area is 2 m<sup>2</sup>. The load–displacement  $p$ – $s$  curve obtained from the shallow plate loading test is shown in Figure 5. It can be seen from Figure 5 that the cumulative settlement of the plate loading is 18.16 mm when loaded to 840 kPa, and the rebound after unloading is 4.66 mm, with a rebound rate of about 25.7%.

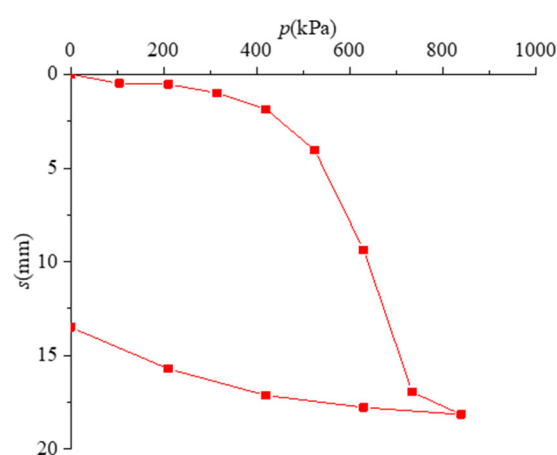


**Figure 5.**  $p$ – $s$  curve by shallow plate loading test in 9# building.

### 3.3. Tangent Modulus Calculation

The plate loading test  $p$ – $s$  curve is fitted by hyperbola  $p = \frac{s}{a + bs}$ . We rewrite the hyperbolic equation into the form of a linear equation  $s/p = bs + a$ . Let  $x = s$ ,  $y = s/p$ ; the linear regression fitting formula is used to obtain:

$$b = \frac{\sum_{i=1}^n (x_i y_i - n \bar{x} \bar{y})}{\sum_{i=1}^n (x_i^2 - n \bar{x}^2)} \quad (6)$$

$$a = \bar{y} - b \bar{x} \quad (7)$$

where  $a, b$  are parameters in the hyperbola;  $x_i, y_i$ , respectively, represent the settlement and the ratio value of settlement to load under different loads; and  $\bar{x}, \bar{y}$  are the average value of  $x_i, y_i$ .

The fitted linear equation is as follows:

$$\frac{s}{p} = 0.0012287s + 0.002607 \quad (8)$$

According to the linear equation,  $a = 0.002607$  and  $b = 0.0012287$ ; the initial tangent modulus  $E_{t0} = 454.84$  MPa can be obtained according to Formula (4). According to the equation  $p_u = 1/b$ , the ultimate bearing capacity of the soil is 813.87 kPa.

In order to verify the effect of the tangent modulus, the load–displacement curve of the pressure plate is now back-calculated using the tangent modulus. The tangent modulus of the gravel layer under different loads was calculated according to the equation

$$E_t = (1 - \frac{P}{P_u})^2 E_{t0}, \text{ and the calculated values of the tangent modulus are shown in Table 4.}$$

It can be seen that the tangent modulus of the soil increases with the increasing of the depth under the same load. In addition, at the same depth, the tangent modulus decreases with the increase of the load.

**Table 4.** Calculation of tangent modulus of gravel layer under various loads.

Soil	Ultimate Bearing Capacity $p_u$ (kPa)	Depth of Soil Layer (m)	Tangent Modulus of Soil Layer under Different Load Levels (MPa)						
			105	210	315	420	525	630	735
gravel layer	814	0.566	343.5	249.3	170.1	106.0	57.0	23.1	4.3
	1264	1.131	394.6	340.4	290.2	244.0	201.8	163.6	129.5
	1714	1.697	428.3	404.4	381.3	358.8	337.0	315.9	295.5
	2163	2.262	441.6	430.6	419.7	408.9	398.3	387.8	377.5
	2613	2.828	447.0	441.2	435.5	429.8	424.2	418.5	413.0
	3063	3.394	449.4	446.1	442.8	439.5	436.2	432.9	429.6
	3513	3.959	450.7	448.7	446.6	444.6	442.6	440.5	438.5
	3963	4.525	451.5	450.1	448.8	447.4	446.1	444.8	443.4
	4413	5.090	451.8	450.7	449.7	448.7	447.6	446.6	445.6
	4863	5.656	452.2	451.5	450.9	450.3	449.7	449.0	448.4
	5313	6.222	452.3	451.8	451.3	450.8	450.3	449.8	449.3
	5762	6.787	452.5	452.1	451.8	451.5	451.1	450.8	450.5
	6212	7.353	452.5	452.3	452.1	451.8	451.6	451.3	451.1
	6662	7.918	452.6	452.5	452.3	452.1	451.9	451.8	451.6
	7112	8.484	452.7	452.6	452.5	452.4	452.3	452.2	452.0

The tangent modulus was used to calculate the settlement under different loads. Figure 6 shows the comparison of the test curve, the hyperbolic fitting curve, and the curve calculated by the tangent modulus method. It can be seen from Figure 6 that the curve calculated by the tangent modulus method is basically consistent with the test curve. It shows that the nonlinear characteristics of the soil settlement can be reflected by the tangent modulus, because the influence of the stress level is taken into account.

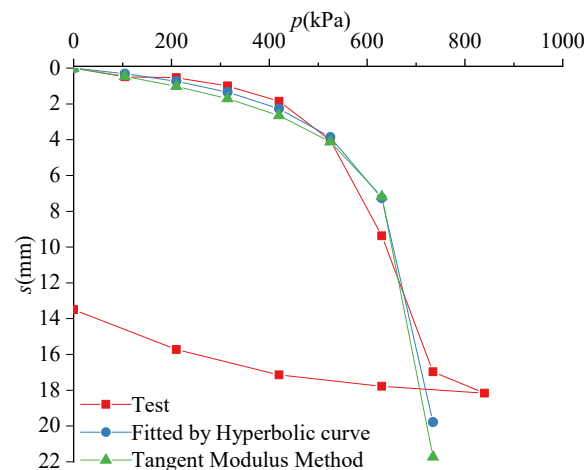


Figure 6. Comparison of  $p$ - $s$  curve.

### 3.4. Settlement Analysis of Composite Foundation under Flexible Uniform Load

Without considering the raft stiffness, the average additional stress coefficient  $\bar{\alpha}$  of the soils at different depth under the flexible uniform load was obtained by looking up the table method [10], and the corresponding additional stress was obtained, and then the settlement of the composite foundation was calculated by the layerwise summation method.

#### 3.4.1. Settlement Calculation Using Modulus of Compression

Under the foundation, there are gravel layer, completely weathered calcareous conglomerate and moderately weathered calcareous conglomerate. The thickness of the gravel layer and the completely weathered calcareous conglomerate are about 8.5 m and 11.3 m, respectively, and the settlement of the moderately weathered conglomerate can be ignored. According to Formula (2), the comprehensive compression modulus of the gravel layer after dynamic compaction can be obtained:

$$E_{sp} = \frac{f_{spk}}{f_{ak}} E_s = \frac{420}{340} \times 27 = 33 \text{ MPa}$$

As the impact of the strong ramming on the lower completely weathered calcareous conglomerate is very small, the compressive modulus of the completely weathered rock is still 15 MPa. The final settlement of the gravel layer  $\Delta s_1$  and the completely weathered rock  $\Delta s_2$  at the raft corner point can be calculated by the layerwise summation method.

$$\Delta s_1 = \frac{p_0}{E_{s1}} z_1 \bar{\alpha}_1 = \frac{336 \times 8.48 \times 0.2455}{33} = 21.20 \text{ mm}$$

$$\Delta s_2 = \frac{p_0}{E_{s2}} (z_2 \bar{\alpha}_2 - z_1 \bar{\alpha}_1) = \frac{336 \times (19.8 \times 0.2214 - 8.48 \times 0.2455)}{15} = 51.56 \text{ mm}$$

The equivalent value of modulus of compression is as follows:

$$\bar{E}_s = \frac{\sum A_i}{\sum \frac{A_i}{E_{si}}} = \frac{p_0 z_2 \bar{\alpha}_2}{\Delta s_1 + \Delta s_2} = \frac{336 \times 19.8 \times 0.2214}{21.20 + 51.56} = 20.24 \text{ MPa}$$

According to the equivalent value of the compression modulus  $\bar{E}_s$  in the calculated depth, the empirical coefficient of the settlement calculation  $\psi_s = 0.25$  is obtained from Table 1, so the corner settlement of the raft foundation is obtained:



$$s_1 = \psi_s (\Delta s_1 + \Delta s_2) = 0.25 \times (21.2 + 51.56) = 18.19 \text{ mm}$$

Similar to the corner point settlement calculation, the calculating settlement  $s_1$  of the midpoint of the raft boundary line is 35.18 mm.

### 3.4.2. Settlement Calculation by Tangent Modulus

- The gravel layer:

The initial tangent modulus  $E_{t0}$  of the gravel layer is 454.84 MPa, and its ultimate bearing capacity  $P_u$  is 813.87 kPa. According to the Technical Code for Ground Treatment of Buildings, the ultimate bearing capacity  $P_u$  of the reinforced foundation is not corrected by width, so the  $P_u$  was only corrected according to the depth, and the tangent modulus of the gravel layer with different stress levels was derived.

- The completely weathered calcareous conglomerate:

According to the Chinese Geological Engineering Handbook [15], the empirical formula of the completely weathered calcareous conglomerate between the deformation modulus and blow count is  $E_0 = 2.2N$ , and the SPT blow count  $N$  of the completely weathered calcareous conglomerate is 16, so the deformation modulus of the weathered calcareous conglomerate is 35.2 MPa [16]. The proportional relationship between the unloading–reloading modulus  $E_{ur}^{\text{ref}}$  and the secant modulus  $E_{50}^{\text{ref}}$  of the completely weathered calcareous conglomerate is  $E_{ur} = 4.3E_{50}$  [17–19]. Assuming that the ratio of the initial tangent modulus to the deformation modulus is the same as the ratio of the unloading–reloading modulus  $E_{ur}^{\text{ref}}$  to the secant modulus  $E_{50}^{\text{ref}}$ , and it can be concluded that the initial tangent modulus  $E_{t0}$  is 151.36 MPa.

The ultimate bearing capacity  $P_u$  of the completely weathered conglomerate is calculated by the Terzaghi formula  $P_u = \frac{1}{2} \gamma b N_\gamma + q N_q + c N_c$ , where  $c$  and  $\phi$  are 32 kPa and  $20^\circ$ , respectively. The tangent modulus of the completely weathered calcareous conglomerate at different depths can be calculated according to Formula (5). Figure 7 shows the  $p$ – $s$  curves of the midpoint and corner of the boundary line calculated by the compression modulus and tangent modulus, respectively, under the uniform load, and the measured curve of corner points 1 and 9 and the midpoint 3 and 7 are presented.

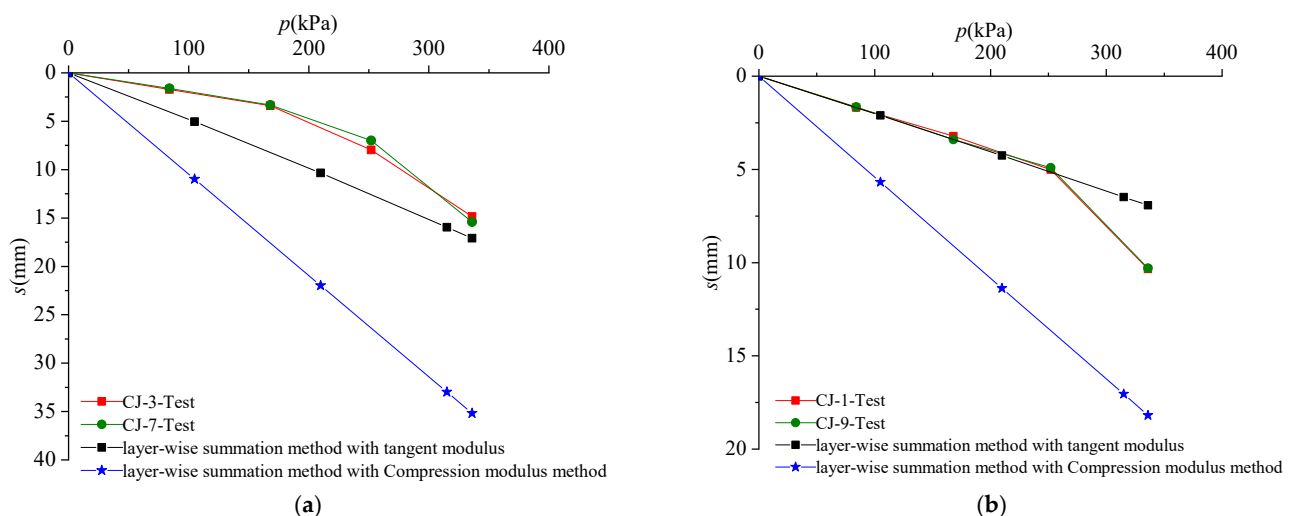


**Figure 7.** Comparison of calculated and measured  $p$ – $s$  curves: (a) midpoint of the boundary line; and (b) corner point.

It can be seen in Figure 7 that the calculated settlements of the corner points and the midpoint by the compression modulus are significantly larger than the measured ones. However, the settlement calculated by the tangent modulus method is very close to the measured, and the corner settlement is slightly smaller than the measured. The reasons may be that the additional stress coefficient is calculated according to the completely flexible load, without considering the influence of raft stiffness.

### 3.5. Finite Element Analysis of Foundation Settlement

#### 3.5.1. Establishment of Finite Element Model

Due to the irregular shape of the raft foundation, the raft model was appropriately simplified as the rectangle in the finite element analysis. According to the symmetry of the structure and load, the 1/4 model was used in the finite element modeling. Ignoring the deformation of the moderately weathered rocks, only the gravel layer and the completely weathered calcareous conglomerate were considered in the finite element model. The thickness of the gravel layer and the completely weathered calcareous conglomerate are 8.5 m and 11.3 m, respectively, and the total thickness of the soil layer is 19.8 m. The total dimensions of the 1/4 finite element model are  $20\text{ m} \times 60\text{ m} \times 19.8\text{ m}$ , and the raft foundation is  $7\text{ m} \times 21.6\text{ m}$ . The bottom boundary of the model is fixed; the lateral normal displacement of the model is constrained, and the tangent displacement is free. The overall finite element model is shown in Figure 8.

The raft was simulated as an elastic model with the elastic modulus 30 GPa, and the soil was simulated as a nonlinear elastic model. The C3D8R element was used for the raft and soil. Surface-to-surface contact was adopted for contact, and small sliding was adopted to track the relative movement of the contact surface. The surface with the larger stiffness was used as the master surface, and the surface with the smaller stiffness was used as the slave surface. In the mechanical model of contact interaction, hard contact was adopted in normal behavior, and a penalty function was adopted in tangential behavior.

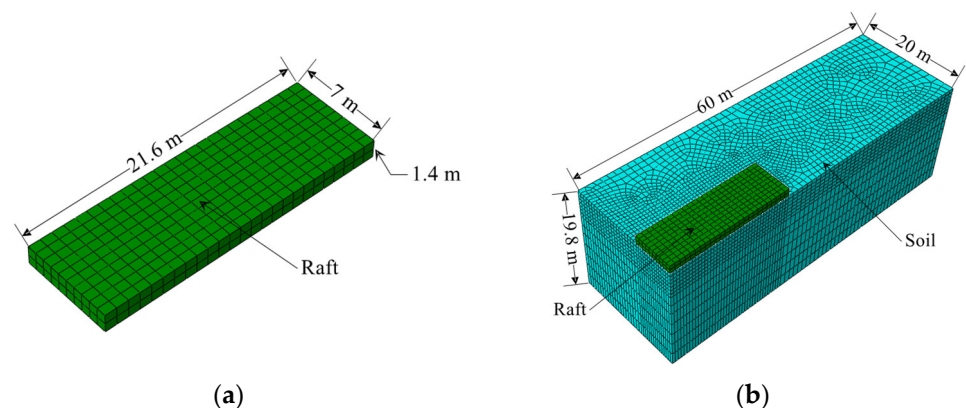
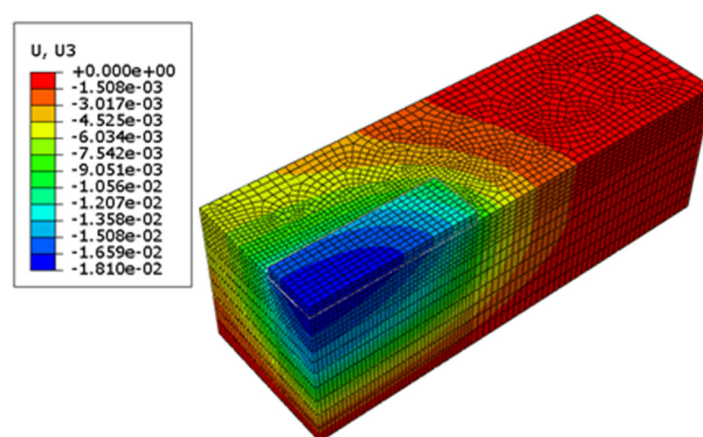


**Figure 8.** Finite element model: (a) raft; and (b) FEM model.

Owing to the fact that the tangent modulus value is affected by the stress level, in ABAQUS2022 software, the field variable can be used to realize the variation of the soil elastic modulus, and different tangent modulus values can be set by the field variable at each loading stage.

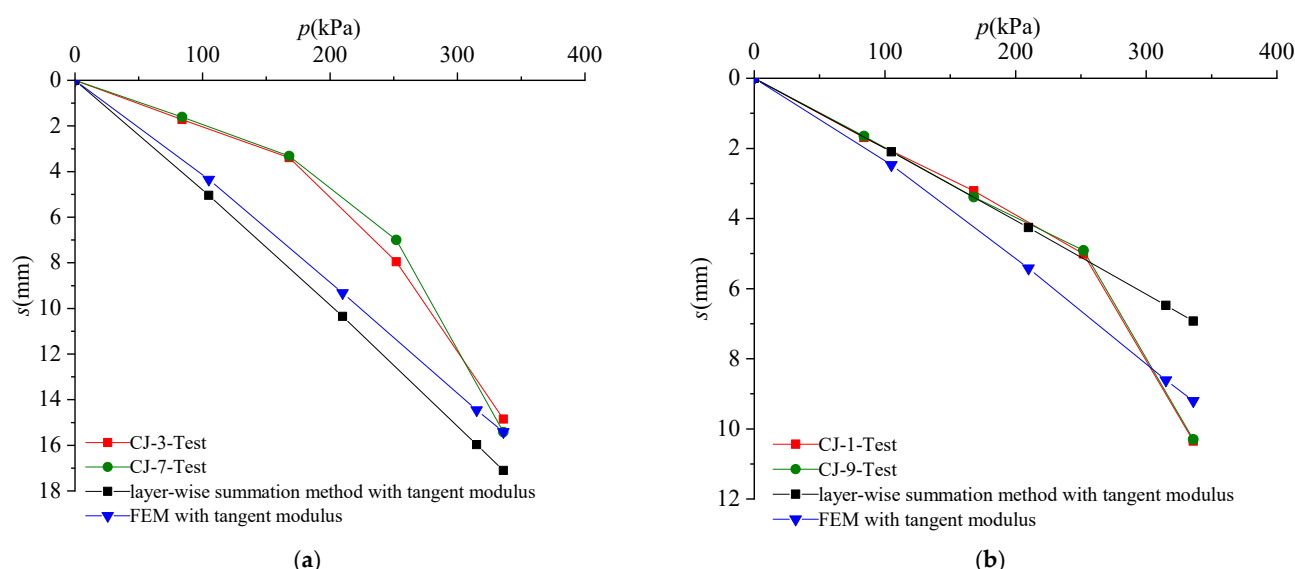
#### 3.5.2. Comparison of the Test and Numerical Results

Figure 9 shows the vertical settlement contour of the raft foundation calculated by using the tangent modulus. It can be seen from Figure 9 that the settlement of the raft foundation shows a disc-shaped distribution, with a large settlement in the middle and a small settlement in the four corners.



**Figure 9.** Vertical settlement contour of raft slab foundation of 9# building (m).

The settlement at the corner points and midpoint of the raft boundary line were extracted and compared with the above. From Figure 10, it can be seen that the simulated settlement by the finite element method (FEM) is also close to the measured value, and the bending stiffness of the raft slab is considered in the FEM.



**Figure 10.** Settlement comparison of  $p$ - $s$  curve: (a) the midpoint of boundary line; and (b) the corner point.

#### 4. Test Case 2—Multi-Layered Soil Foundation with Rigid Pile

##### 4.1. Project Profile

The 15# building is also a high-rise residential building with 28 floors above ground and one basement. The typical geological profile is shown in Figure 11, and the 1.4 m thick raft is located at  $-4.44$  m. Figure 12 shows the layout of the shear wall and the border of the raft and composite foundation. The raft foundation is an irregular plane, and the length and width of the raft foundation are 92.45 m and 27.95 m, respectively.

Because the thinnest part of the gravel layer under the raft foundation is only 2.5 m, which is far less than the thickness of the gravel layer of the 9# building, a concrete rigid pile composite foundation was adopted to meet the requirements of the bearing capacity and the deformation of building. The rigid pile diameter is 0.6 m, with moderately weathered rocks as the bearing layer, and the adjacent rigid pile spacing is 3 m. The cushion with a thickness of 0.5 m was laid on the top of the composite foundation.

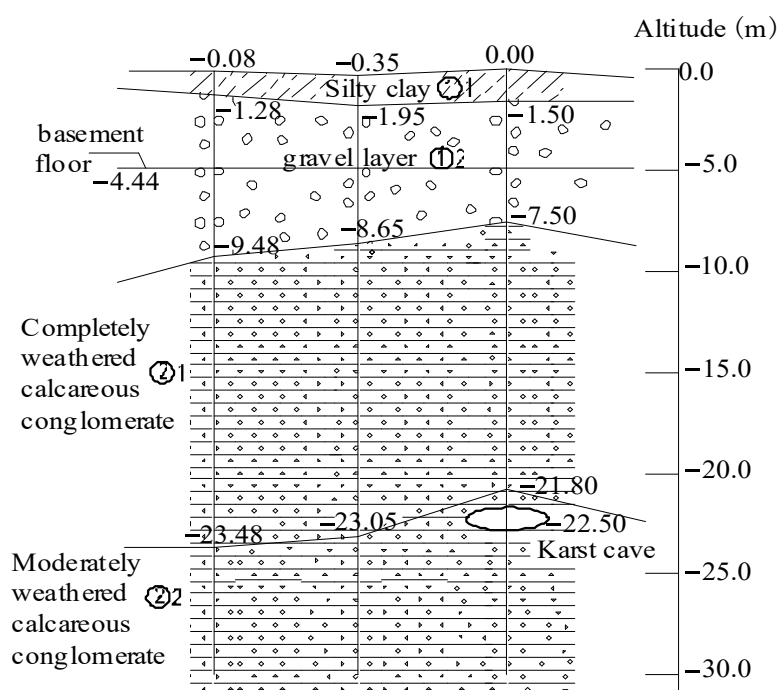


Figure 11. Typical geological profile of 15# building.

According to the Chinese Code for Deformation Measurement of Building and Structure [15], 10 monitoring points were placed around the building for settlement monitoring, and the monitoring points were arranged on the shear wall of the structure. Table 5 shows the settlement values of the monitoring points for construction up to the 7th, 14th, 21st, and 28th floors, respectively, and the settlement in the table does not include post-construction settlement. The load of each floor of the structure during construction is about 12 kN/m<sup>2</sup>.

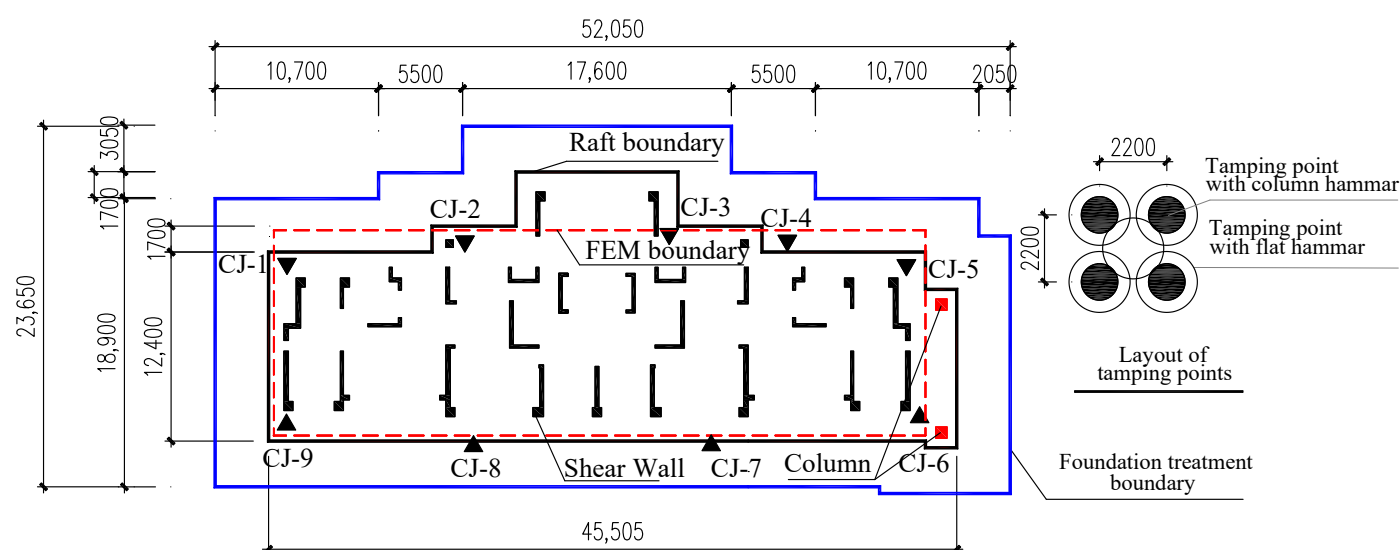


Figure 12. Shear wall and foundation plan layout of 15# building.

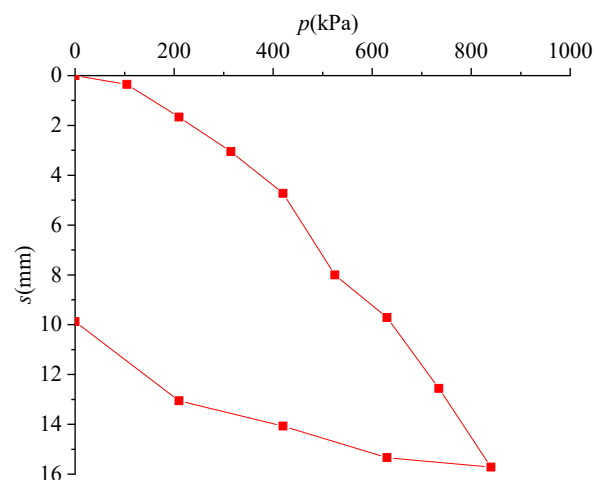
**Table 5.** Settlement of monitoring point.

Monitoring Point	Cumulative Settlement (mm)			
	Construction to the 7th Floor (84 kN/m <sup>2</sup> )	Construction to the 14th Floor (168 kN/m <sup>2</sup> )	Construction to the 21st floor (252 kN/m <sup>2</sup> )	Construction to the 28th Floor (336 kN/m <sup>2</sup> )
CJ-1	2.04	3.15	6.19	12.30
CJ-2	2.13	3.19	6.82	13.79
CJ-3	2.11	3.13	6.47	13.31
CJ-4	2.16	3.18	6.71	13.96
CJ-5	2.09	3.16	6.64	13.62
CJ-6	2.12	3.28	6.65	14.04
CJ-7	2.18	3.26	6.69	13.77
CJ-8	2.16	3.26	6.3	14.25
CJ-9	2.13	3.25	6.54	14.74
CJ-10	2.06	3.12	6.48	13.93

#### 4.2. Vertical Static Load Test of Soil

Figure 13 shows the  $p$ - $s$  curve of the soil by shallow plate loading test. It can be seen that the cumulative settlement is 15.72 mm when loaded to 840 kPa, and the rebound after unloading is 5.72 mm, with a rebound rate of about 36.3%.

The  $p$ - $s$  curve fitting equation is  $s/p = 0.000908s + 0.006$ , where  $a = 0.006$  and  $b = 0.000908$ . The initial tangential modulus  $E_0$  of the gravel layer is 197.66 MPa, and the ultimate bearing capacity  $P_u$  of the gravel layer is 1101.32 kPa.

**Figure 13.**  $p$ - $s$  curve by shallow plate loading test in 15# building.

#### 4.3. Finite Element Analysis of Foundation Settlement

##### 4.3.1. Establishment of Finite Element Model

Due to the irregular shape of the raft foundation, the raft model was appropriately simplified as the rectangle in the finite element analysis. According to the symmetry of the structure and load, the 1/4 model was used in the finite element modeling. Due to the large elastic modulus of the moderately weathered calcareous conglomerate, only the cushion, the gravel layer, and the completely weathered calcareous conglomerate were considered in the finite element model. In addition, the thickness of the cushion is 0.5 m, and the thickness of the gravel layer and the completely weathered calcareous conglomerate are 5 m and 11 m, respectively. The total thickness of the soil layer is 16.5 m. The total dimensions of the 1/4 finite element model are 32 m  $\times$  62.5 m  $\times$  16.5 m, and the 1/4 raft foundation is 8 m  $\times$  38.5 m. The bottom boundary of the model was fixed. The lateral

normal displacement of the model is constrained, and the tangent displacement was free. The overall finite element model is shown in Figure 14.

The raft and rigid pile were simulated as an elastic model with the elastic modulus 30 GPa, and the cushion was simulated by a Mohr–Coulomb constitutive model with the elastic modulus 60 MPa. The soil was simulated as a nonlinear elastic model. The C3D8R elements were used for the platform, rigid pile, cushion, and soil. The contact element was used to simulate the rigid pile and the soil, the rigid pile and cushion, and the raft and cushion. Surface-to-surface contact was adopted for contact. Small sliding was adopted to track the relative movement of the contact surface. The surface with the larger stiffness was used as the master surface, and the surface with the smaller stiffness was used as the slave surface. In the mechanical model of contact interaction, hard contact was adopted in normal behavior, and the penalty function was adopted in tangential behavior.

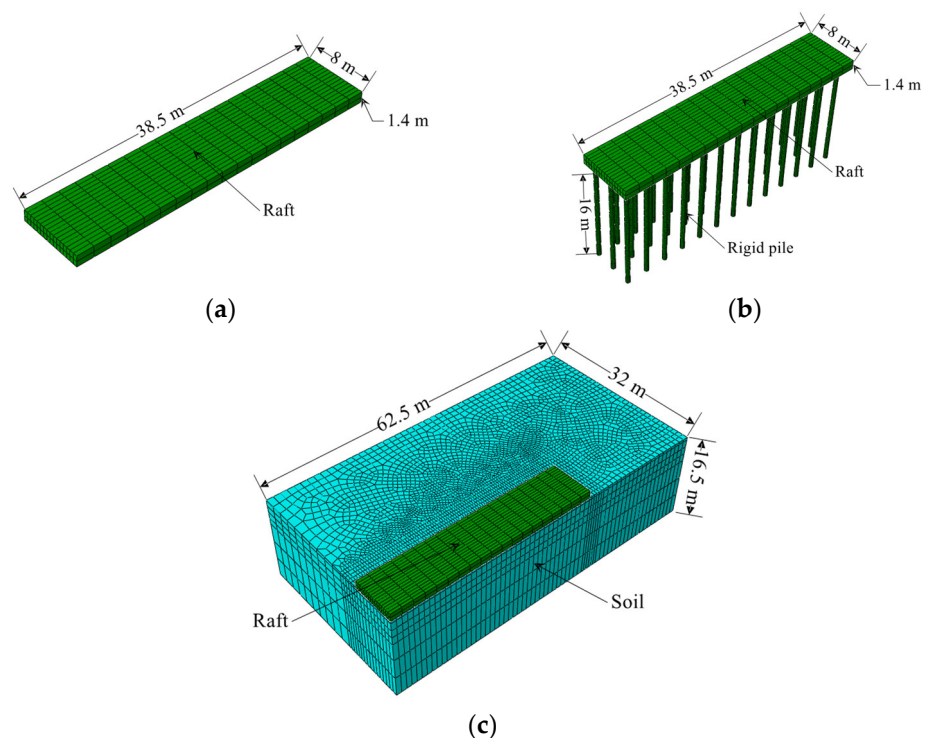


**Figure 14.** Finite element model of rigid pile composite foundation of Building 15: (a) raft; (b) raft and pile; and (c) FEM model.

#### 4.3.2. Comparison of the Test and Numerical Results

Figure 15 shows the vertical settlement contour of the rigid pile composite foundation of the 15# building. Compared with the settlement deformation contour of the 9# building, it can be seen that the disc deformation effect of the settlement was significantly smaller. The main reason is that the deformation of the 15# building is affected by the combined effect of the pile and soil deformation. The deformation of the soil is in accordance with the Boussinesq solution under the flexible load, showing an obvious disc deformation effect. While the deformation characteristic of the end-bearing rigid pile is similar to the independent spring of the Winkler model, the settlement of the  $i$ th rigid pile is only related to the stress acting on the  $i$ th rigid pile, and is not related to the stress on the other rigid piles, so the deformation of the 15# building shows a smaller disc deformation effect.



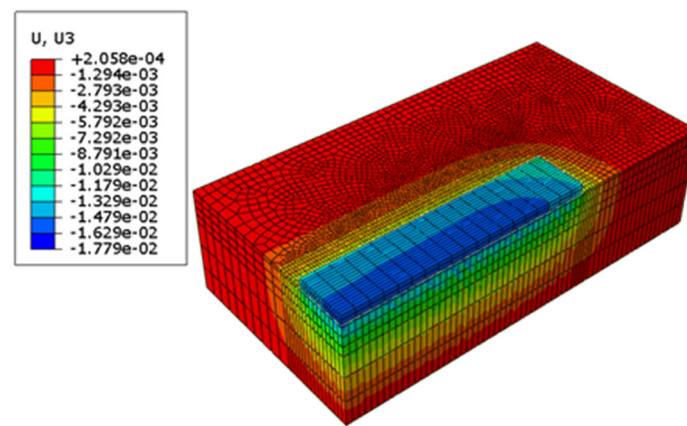


**Figure 15.** Vertical settlement contour of rigid pile composite foundation (m).

Figure 16 shows the comparison between the calculated settlement and the measured settlement. It can be seen from Figure 16 that the calculated settlement at the midpoint of the boundary line is close to the measured settlement. The measured curve shows an obvious nonlinear phenomenon, while the calculated curve shows no obvious nonlinear phenomenon. After the completion of the 28th floor, the measured settlement of the midpoint of the foundation sideline is basically consistent with the calculated settlement, but the calculated settlement of the corner point is slightly smaller than the measured settlement.

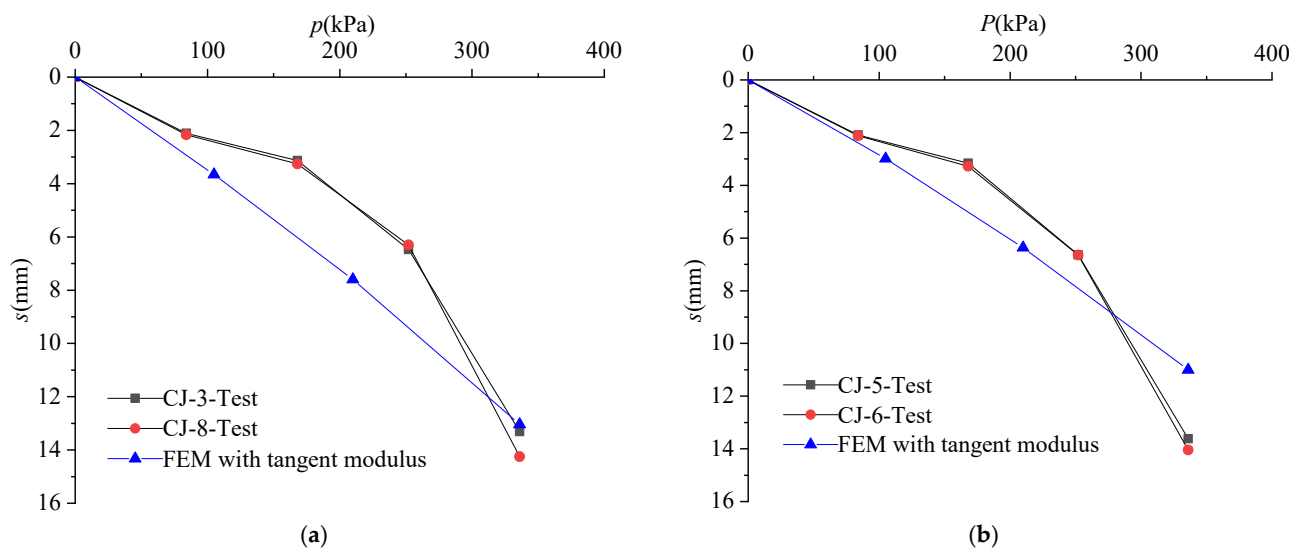


**Figure 16.** Comparison of finite element and measured  $p$ – $s$  curves: (a) the midpoint of the boundary line; and (b) the corner point.

The vertical stress contour of the rigid pile and soil is shown in Figure 17. From Figure 17a, it can be seen that the stress at the top of the rigid pile is about 4.7 MPa, and the vertical stress of the rigid pile increases gradually with the depth. Because the coefficient of the friction of the upper gravel layer is greater than that of the completely weathered calcareous conglomerate, and the upper soil layer has a higher additional stress, the stress in the upper part of the rigid pile grows faster. It can be seen from Figure 17b that the soil average stress between piles is about 240 kPa, and the pile–soil stress ratio is approximately 19.6, which is in an ideal state.

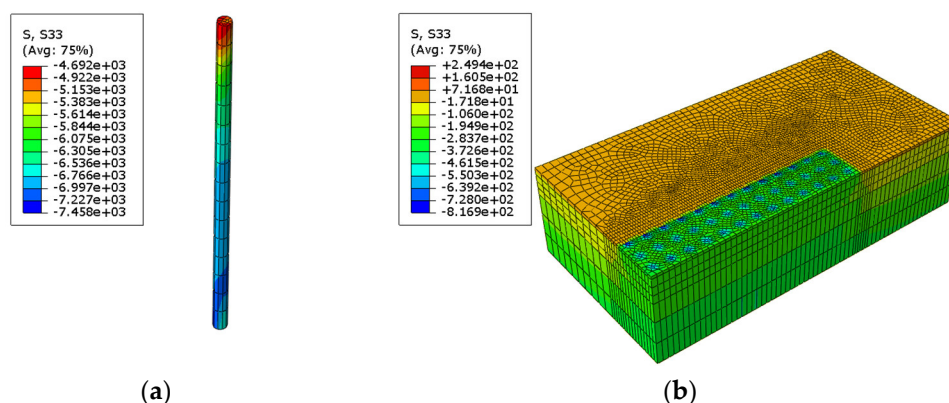


Figure 17. Vertical stress contour (kPa): (a) rigid pile; and (b) soil.

## 5. Conclusions

In this paper, the tangent modulus was used to calculate and analyze the settlement of the composite foundations of two high-rise buildings, and the calculated settlement is compared with the measured results. The main conclusions are as follows:

- (1) The tangent modulus method is mainly suitable for the hard plastic soil with a strong structure, such as silty clay, completely weathered rock, granite residual soil, and so on, whose SPT blow count  $N$  is more than 8.
- (2) The tangent modulus takes into account the influence of soil stress and can better reflect the nonlinear settlement characteristics of the foundation. The measured settlement results of the two cases show that the calculation accuracy of the tangent modulus is significantly better than the traditional compression modulus.
- (3) The Chinese foundation code adopts the empirical coefficient of the settlement calculation to adjust the settlement of low-compressibility soil, and the minimum empirical coefficient of the settlement is 0.2. However, the value of the empirical coefficient is greatly influenced by the experience of the engineers. The tangent modulus method directly obtains the tangent modulus of the soil by an in-situ pressure plate test, and no empirical coefficient is needed in the settlement calculation process.
- (4) Owing to the high cost of the deep plate load test, for deep hard plastic soil, it is a common geological exploration method to determine the deformation modulus of deep soil by the SPT blow count, and there are corresponding empirical formulae for different types of soil in different regions. In this paper, it is assumed that the ratio of the initial tangential modulus to the deformation modulus is the same as the ratio of the unloading and reloading modulus  $E_{ur}^{ref}$  to the secant modulus  $E_{50}^{ref}$  obtained from the triaxial test of the sampled soil, and then the initial tangential modulus can be derived from this ratio. The related method can greatly reduce the cost of obtaining the tangent modulus of deep soil. The analysis results of two cases prove that the method has high accuracy. More deep plate loading tests are required to further verify whether the method is universal.

**Author Contributions:** Conceptualization, Y.L., X.L. and L.Y.; methodology, Y.L.; software, G.C. and W.Z.; validation, Y.L., G.C. and L.Y.; formal analysis, Y.L., G.C., W.Z. and L.Y.; resources, Y.L. and L.Y.; data curation, G.C., L.Y. and W.Z.; writing—original draft preparation, G.C., W.Z. and L.Y.; writing—review and editing, Y.L., L.Y., G.C. and W.Z.; visualization, Y.L., G.C. and W.Z.; supervision, L.Y.; project administration, Y.L.; funding acquisition, Y.L. and X.L. All authors have read and agreed to the published version of the manuscript.

**Funding:** This research was funded by JiangXi Jiye Science and Technology Group Co., Ltd. [Grant No. 2020001].

**Institutional Review Board Statement:** Not applicable.

**Informed Consent Statement:** Not applicable.



**Data Availability Statement:** The data used to support the findings of this study are available from the authors upon request.

**Conflicts of Interest:** The authors declare that they have no conflict of interest to report regarding the present study.

## References

1. Zhang, L.; Zhao, M.H.; Shi, C.J.; Zhao, H. Settlement Calculation of Composite Foundation Reinforced with Stone Columns. *Int. J. Geomech.* **2013**, *13*, 248–256.
2. Chang, D.W.; Lu, C.W.; Tu, Y.J.; Cheng, S.H. Settlements and Subgrade Reactions of Surface Raft Foundations Subjected to Vertically Uniform Load. *Appl. Sci.* **2022**, *12*, 5484.
3. Pantelidis, L. Empirical Relationships Between the Elastic Settlement of Rigid Rectangular Foundations and the Settlement of the Respective Flexible Foundations. *Geotech. Geol. Eng.* **2021**, *39*, 3959–3971.
4. Wang, J.; Ji, H.G.; Wang, C.Q.; Bai, Y. Analysis the Settlement Calculation Methods of Combined Piles in Composite Foundation. *Appl. Mech. Mater.* **2011**, *71–78*, 28–31.
5. Yang, G.H. Nonlinear settlement computation of the soil foundation with the undisturbed soil tangent modulus method. *Chin. J. Geotech. Eng.* **2006**, *28*, 1927–1931. (In Chinese)
6. Duncan, J.M.; Chang, C.Y. Nonlinear Analysis of Stress and Strain in Soils. *J. Soil Mech. Found. Div.* **1970**, *96*, 1629–1653.
7. Yang, G.H.; Wang, P.; Qiao, Y. An undisturbed-soil secant modulus method for calculation of nonlinear settlement of soil foundations. *China Civ. Eng. J.* **2007**, *40*, 49–52. (In Chinese)
8. Yang, G.H. New computation method for soil foundation settlements. *Chin. J. Rock Mech. Eng.* **2008**, *27*, 679–686. (In Chinese)
9. Peng, C.X.; Yang, G.H. A simplified method for determining e-p curve of soft soil and its application to analyzing nonlinear settlement of foundation. *Rock Soil Mech.* **2008**, *29*, 1706–1710. (In Chinese)
10. GB50007-2011; Code for Design of Building Foundation. China Architecture & Building Press: Beijing, China, 2011.
11. JGJ79-2012; Technical Code for Ground Treatment of Buildings. China Architecture & Building Press: Beijing, China, 2012.
12. Vakili, K.N.; Barciaga, T.; Lavasan, A.A.; Schanz, T. A practical approach to constitutive models for the analysis of geotechnical problems. *Third Int. Symp. Comput. Geomech.* **2013**, *1*, 738–749.
13. Mohsan, M.; Vardon, P.J.; Vossepoel, F.C. On the use of different constitutive models in data assimilation for slope stability. *Comput. Geotech.* **2021**, *138*, 104332.
14. Wu, J.T.H.; Tung, S.C.-Y. Determination of Model Parameters for the Hardening Soil Model. *Transp. Infrastruct. Geotechnol.* **2019**, *7*, 55–68.
15. JGJ8-2007; Code for Deformation Measurement of Building and Structure. China Architecture & Building Press: Beijing, China, 2007.
16. Hua, J.X.; Zheng, J.G. *Geological Engineering Handbook*, 5th ed.; China Architecture & Building Press: Beijing, China, 2018; pp. 206–223.
17. Zhu, M.; Chen, X.S.; Zhang, G.T.; Pang, X.C.; Su, D.; Liu, J.Q. Parameter back-analysis of hardening soil model for granite residual soil and its engineering applications. *Rock Soil Mech.* **2022**, *43*, 1061–1072. (In Chinese)
18. Luo, M.M.; Chen, Y.; Zhou, J. Research status and prospect of parameter selection for the HS-small model. *Ind. Constr.* **2021**, *51*, 172–180. (In Chinese)
19. Liu, W.H.; Zhu, H.; He, S.J.; Yan, J.B.; Xu, C.J. Experimental study on parameters of hardening soil model for soils and its application in foundation pit engineering in Nanchang. *J. Civ. Environ. Eng.* **2021**, *43*, 38–47. (In Chinese)

**Disclaimer/Publisher's Note:** The statements, opinions and data contained in all publications are solely those of the individual author(s) and contributor(s) and not of MDPI and/or the editor(s). MDPI and/or the editor(s) disclaim responsibility for any injury to people or property resulting from any ideas, methods, instructions or products referred to in the content.